Clim Dyn
DOI 10.1007/s00382-007-0234-0

Impacts of recent El Niño Modoki on dry/wet conditions in the Pacific rim during boreal summer

Hengyi Weng · Karumuri Ashok · Swadhin K. Behera · Suryachandra A. Rao · Toshio Yamagata

Received: 14 August 2006 / Accepted: 31 January 2007

Abstract Present work uses 1979–2005 monthly observational data to study the impacts of El Niño Modoki on dry/wet conditions in the Pacific rim during boreal summer. The El Niño Modoki phenomenon is characterized by the anomalously warm central equatorial Pacific flanked by anomalously cool regions in both west and east. Such zonal SST gradients result in anomalous two-cell Walker Circulation over the tropical Pacific, with a wet region in the central Pacific. There are two mid-tropospheric wave trains passing over the extratropical and subtropical North Pacific. They contain a positive phase of a Pacific-Japan pattern in the northwestern Pacific, and a positive phase of a summertime Pacific-North American pattern in the northeastern Pacific/North America region. The western North Pacific summer monsoon is enhanced, while the East Asian summer monsoon is weakened. In the South Pacific, there is a basin-wide low in the mid-latitude with enhanced Australian high and the eastern South Pacific subtropical high. Such an atmospheric circulation pattern favors a dry rim surrounding the wet central tropical Pacific. The El Niño Modoki and its climate impacts are very different from those of El Niño. Possible geographical regions for dry/wet conditions influenced by El Niño Modoki and El Niño are compared. The two phenomena also have very different temporal features. El Niño Modoki has a large decadal background while El Niño is predominated by interannual variability. Mixing-up the two different phenomena may increase the difficulty in understanding their mechanisms, climate impacts, and uncertainty in their predictions.

Keywords El Niño Modoki · El Niño · Climate extremes · Boreal summer teleconnections · The Pacific rim

H. Weng · K. Ashok · S. K. Behera · S. A. Rao · T. Yamagata
Frontier Research Center for Global Change/JAMSTEC, Yokohama, Japan

T. Yamagata
Department of Earth and Planetary Science, Graduate School of Science, University of Tokyo, Tokyo, Japan

H. Weng (✉)
Climate Variations Research Program, Frontier Research Center for Global Change, JAMSTEC, Yokohama 236-0001, Japan
e-mail: weng@jamstec.go.jp; hengi_wang@yahoo.com

1 Introduction

The summers of 1994, 2002, and 2004 were identified as the El Niño summers based on the Niño3.4 index by the Climate Prediction Center of NOAA, USA[1]. However, the sea surface temperature (SST) distribution in the tropical Pacific in these events had a common feature that was not typical during the canonical El Niño. The warmest SST anomalies (SSTA) during these events were maintained in the central equatorial Pacific with cooler SSTA in both east and west, while the warmest SSTA during the canonical El Niño events appears in the eastern equatorial Pacific (Yamagata et al. 2004; McPhaden 2004; WMO 2005 in http://www.wmo.int/index-en.html). Moreover, the teleconnection patterns in these events were also very different from those related to the canonical El Niño. For example, during El Niño summers, much of the Japan Sea side in the southern Japan and much of the western USA tend to have

[1] http://www.cpc.ncep.noaa.gov/products/analysis_monitoring/enso-stuff/ensoyears.shtml

above-normal rainfall and/or below-normal temperature[2]. The tropical storm activity over western North Pacific is displaced southeastward so that there would be less typhoon activity near Japan (Chan 2000; Saunders et al. 2000; Chia and Roplewski 2002). On the contrary, in the summer of 2004, for example, much of Japan experienced droughts due to lack of rainfall and record-breaking high temperature. Meantime, a record-breaking number of ten typhoons landed on Japan in that typhoon season; six of them made landfall in that summer[3]. These typhoons brought abundant rainfall to the Nansei Islands and the Pacific Ocean side of the southwestern Japan causing local floods (Kim et al. 2005). Half a globe away, the 2004 Atlantic tropical storm activity was also unusually high. The August of 2004 had eight named storms forming over the Atlantic in a single month. Four hurricanes hit a single state (Florida) in the 2004 hurricane season[4] (June–November), which is not the case during El Niño (Gray 1984). Moreover, the western North America from Alaska to California suffered from droughts. Some areas in the western USA experienced *persistent* severe drought in the beginning of the twenty-first century. Persistent droughts were also observed in northern and eastern Australia almost in the same period; the year of 2002 was the fourth driest year on record (Coughlan et al. 2004). Apparently, these persistent regional climate extremes cannot be explained by canonical El Niño or La Niña teleconnection patterns. As will be shown later, these extremely dry and wet conditions are very likely related to an unusual tropical SSTA pattern, known in Japan as El Niño Modoki (or Pseudo El Niño) coupled ocean–atmosphere phenomenon[5] (Ashok et al. 2007).

Since the El Niño Modoki phenomenon is characterized by above-normal SST in the central equatorial Pacific flanked by below-normal SST in both east and west, there is negative (positive) zonal SST gradient in the eastern (western) tropical Pacific. The El Niño Modoki phenomenon is quantified by an El Niño Modoki Index (EMI) constructed by Ashok et al. (2007). The index captures the zonal SST gradients in both eastern and western tropical Pacific.

The roles of along-equator SST gradient in the intensity and the longitudinal position of the Walker Circulation were discussed by Bjerknes (1969), which has large influence on precipitation in the Pacific region. Lindzen and Nigam (1987) used their model experiments to show that a large fraction of the total convergence in the central and western tropical Pacific is due to the zonal SST gradient, which is the major contributor to observed precipitation anomalies. Modeling studies have confirmed that precipitation anomalies are primarily associated with anomalous low-level moisture convergence (e.g., Shukla and Wallace 1983). Thus, anomalous atmospheric circulations that are directly or indirectly forced by anomalous tropical zonal SST gradients and the associated low-level moisture convergence are the links between the moisture source in the tropical Pacific and the precipitation anomalies in the Pacific rim countries.

The canonical El Niño phenomenon has already been extensively studied. The research topics on El Niño vary widely from the observational analyses (e.g., Rasmusson and Carpenter 1982; Wallace et al. 1998; Rasmusson 1991; Larkin and Harrison 2005) to modeling studies (e.g., Zebiak and Cane 1987; Xie 1995; Neelin et al. 1998; Kang and Kug 2002). However, to quantify an El Niño event itself is still a problem, because the term ''El Niño'' has been used for different physical meanings (Trenberth 1997; Trenberth and Stepaniak 2001; Larkin and Harrison 2005). It is no wonder that various El Niño indices were proposed[6] since Rasmusson and Carpenter (1982).

El Niño events are in general identified based on a single area-averaged SSTA in the eastern or central equatorial Pacific. It is possible that any equatorial Pacific ocean-atmosphere coupled phenomena that satisfy the criterion of a specified El Niño index, such as the Niño3.4 index, could be identified as ''El Niño'' events. However, this objective method identifies an El Niño event despite that the maximum SSTA is either in the eastern equatorial Pacific (~Niño3 area) or in the central equatorial Pacific (~Niño4 area), and disregard whether the SST gradient in the eastern or western equatorial Pacific is positive or negative. Thus, some events that did not have the features of the canonical El Niño have been classified as El Niño based on the Niño3.4 index. For example, the period of 1990–1995 was previously identified as a prolonged El Niño-Southern Oscillation (ENSO) event by Trenberth and Hoar (1996). Interestingly, they did find that in the canonical El Niño region (the eastern equatorial Pacific) SSTA had waxed and waned, while the SSTA in the central equatorial Pacific in the Niño4 region remained positive from 1990 to June 1995. Although they concluded that the prolonged warming event was something different from the canonical El Niño, they did not classify it into a phenomenon which is different from El Niño. In a very interesting paper about the evolution of the 2002–2003 El Niño, McPhaden (2004) found some peculiar spatial characteristics: the maximum

[2] http://www.data.kishou.go.jp/climate/elnino/tenkou/sekai1.html

[3] http://www.data.kishou.go.jp/climate/cpdinfo/monitor/2004/2_1.html

[4] http://en.wikipedia.org/wiki/2004_Atlantic_hurricane_season

[5] http://www.japantimes.co.jp/cgi-bin/getarticle.pl5?nn20040724f3.htm

[6] The definitions of some commonly used El Niño indices, such as Niño1+2, Niño3, Niño4, and Niño3.4 can be found in many references, e.g., http://www.cpc.ncep.noaa.gov/products/analysis_monitoring/bulletin/table2.html.

SSTA was maintained in the central equatorial Pacific that was different from the canonical El Niño. Similar feature was found in the 2004–2005 event (Ashok et al. 2007).

As will be shown in the present paper, the rainfall anomalies in some Pacific rim countries associated to these events were very different from those to the canonical El Niño events. Thus, the 1994–1995, 2002–2003, and 2004–2005 events should be classified into El Niño Modoki events rather than El Niño events. It would otherwise be difficult to recognize and understand different climate impacts and teleconnection patterns related to these events. Mixing-up the two different phenomena may increase the difficulty in understanding their global and regional climate impacts and uncertainty in their predictions.

The purpose of this work is to explore the teleconnection paths between the SSTA in the equatorial Pacific and the extremely dry/wet conditions in some Pacific rim countries during El Niño Modoki summer, which are distinguished from those during El Niño summer. The material is arranged as follows. Section 2 describes the data and methods we use. Section 3 introduces the unique spatial and temporal characteristics of El Niño Modoki. Section 4 discusses anomalous upper-level and vertical atmospheric circulations as part of teleconnection paths. Section 5 compares different features of the mid- and lower-tropospheric circulations and related rainfall anomalies between El Niño Modoki and El Niño. Section 6 discusses some issues and caveats and makes concluding remarks.

2 Data and methods

We make use of multiple datasets in this study for the period from January 1979 through December 2005: monthly datasets of SST from HadISST (Rayner et al. 2003), atmospheric fields from the NCEP/NCAR Reanalysis data (Kalnay et al. 1996), and rainfall from the Global Precipitation Climatology Project (GPCP) Version 2 Combination data (Adler et al. 2003). Although the GPCP precipitation data set is good for open oceans (Yu and McCreary 2004; Yin et al. 2004), it does not provide the information as detail as we would like to have for some Pacific rim countries. Thus, additional in-situ rainfall data for the USA, Japan, and China are also used in the analyses.

For background knowledge, Fig. 1 gives some of the climatological mean fields averaged for 1979–2005 boreal summers (June–July–August, or JJA). Figure 1a shows the mean fields of SST, 200 hPa velocity potential and divergent velocity, and Fig. 1b shows the mean fields of 500 hPa geopotential height (gph), 850 hPa horizontal wind, and the precipitation rate. The regions for the two monsoon systems in East Asia/western Pacific that will be discussed in this paper are defined as follows: the western North Pacific summer monsoon is in the region (110°–170°E, 7°–20°N), and the East Asian summer monsoon is in the region (110°–140°E, 20°–45°N)[7]. All the anomalies discussed in this paper are departures from their respective means during this period.

Following Ashok et al. (2007), the El Niño Modoki index or EMI is defined as

$$\mathrm{EMI} = [\mathrm{SSTA}]_{\mathrm{C}} - 0.5[\mathrm{SSTA}]_{\mathrm{E}} - 0.5[\mathrm{SSTA}]_{\mathrm{W}}, \qquad (1)$$

where the square bracket with a subscript represents the area-mean SSTA, averaged over one of the three regions specified as the central (C: 165°E–140°W, 10°S–10°N), eastern (E: 110°–70°W, 15°S–5°N), and western (W: 125°–145°E, 10°S–20°N). These regions are marked in Fig. 2a.

The choice of using the three regions to define the EMI has been justified by Ashok et al. (2007). It is based on the second mode of an empirical orthogonal functions (EOF) analysis of the tropical Pacific SSTA between 30°S and 30°N for the period of 1979–2004. The spatial features of the two leading modes, EOF1 and EOF2, look like those of the canonical El Niño and El Niño Modoki, respectively. The principal components of the two leading modes, PC1 and PC2[8], have very high correlations with the Niño3 index (0.98) and the EMI (0.91), respectively. Here, the Niño3 index is defined by the mean SSTA averaged over the region (150°–90°W, 5°S–5°N), as marked in Fig. 2b. Since the EMI and the Niño3 index are highly correlated, respectively, to PC1 and PC2 while the correlation between PC1 and PC2 is zero, the correlation between the Niño3 index and the EMI is very low (0.13). As a common practice, for the convenience of calculation we use the Niño3 index and the EMI instead of PC1 and PC2.

While studying the climate impacts of El Niño Modoki phenomenon, we isolate the impacts from El Niño that is quantified by the Niño3 index here (or simply as ''Niño3''). Most teleconnections between anomaly fields and the EMI or the Niño3 index are studied through their

[7] There are different definitions about the regions of the western North Pacific summer monsoon and the East Asian summer monsoon (Tao and Chen 1987; Wang and Lin 2002; Ding and Chan 2005). Here we use the definitions by Wang and Lin (2002).

[8] Trenberth and Stepaniak (2001), based on the PC2 from a similar EOF analysis, defined an index called *the Trans-Niño index (TNI)* by the difference between the normalized SST anomalies averaged in the Niño1+2 and Niño4 regions. The TNI does not include the zonal SST gradient in the western equatorial Pacific. The main difference between the TNI and EMI is in their concepts. The TNI, just as its name implies, ''*capture the evolution of ENSO in the months leading up to the event and, with opposite sign, the subsequent evolution after the event*''. As shown in this work, the El Niño Modoki phenomenon is not necessarily a stage of a developing or decaying ENSO cycle.

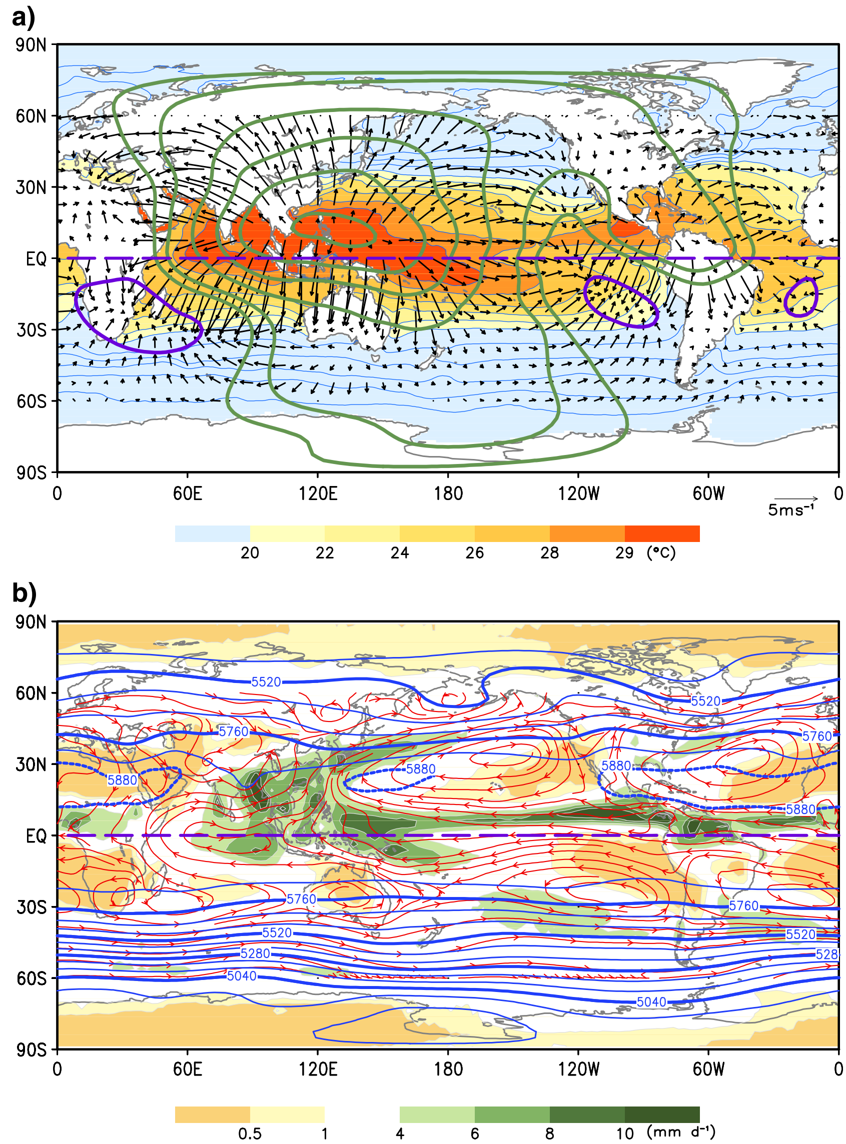

Fig. 1 Summer season (Jun–Jul–Aug, JJA) mean fields for the period of 1979–2005 of **a** SST (*shading*), divergent wind (*arrow*), and 200 hPa velocity potential (contours: *green*/*purple* for negative/positive values at –20 –16, –12, –8, –4, –2, 2 10^5 m^2 s^{-1}), and **b** GPCP precipitation rate (*shading*), 500 hPa geopotential height (*blue contours*; unit: m) and 850 hPa horizontal wind (*red streamlines*)

partial correlation or partial regression patterns while keeping the other index unchanged (Behera and Yamagata 2003; Ashok et al. 2007). Since our purpose is to study only the climate impacts from the tropical Pacific ocean–atmosphere phenomena, the impacts from other phenomena (e.g., the Arctic Oscillation, the Indian Ocean Dipole) are not considered here.

All the statistical significance tests for partial correlations and regressions are performed using the two-tailed Student's *t* test. The degrees of freedom used for such a test are 25 for a time series having 27 summers[9]. The correlation coefficients at significance levels 80, 90, and 95% are 0.25, 0.32 and 0.38, respectively. Composite analysis is also used with the similar significance test; the degrees of freedom are (*N*-1) where *N* is the number of summers to be composed. To study the temporal characteristics of each index, we also use the Morlet wavelet transform (Weng and Lau 1994; Lau and Weng 1995). For simplicity, the terms ''summer'', ''wet (dry)'', ''high (low)'' used in the text are in fact for ''boreal summer'', ''wetter (drier) than normal'', or ''higher (lower) than normal'', respectively. Here, the term ''normal'' is for the ''climatological mean'' during this data period. The term ''El Niño'' is used for the canonical El Niño defined by the Niño3 index, if not specified otherwise.

3 Spatial and temporal features of El Niño Modoki

3.1 Spatial features and some teleconnections

The main spatial features of El Niño Modoki and El Niño are studied by comparing their respective SST and atmospheric anomaly fields. In Fig. 2, we compare the com-

[9] http://www2.chass.ncsu.edu/garson/pa765/partialr.htm

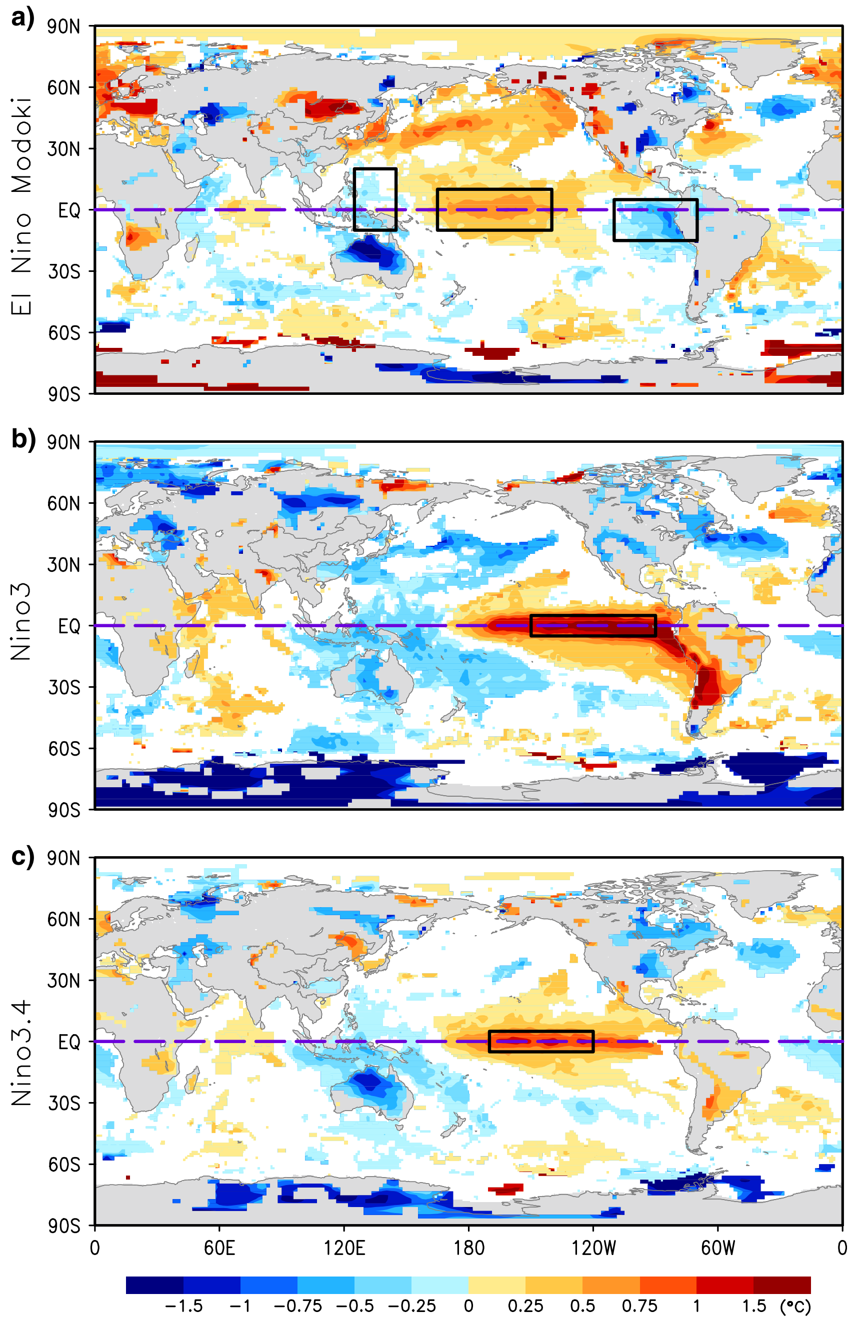

Fig. 2 Composites of summer SSTA over oceans and skin temperature anomalies over land for the three largest events of **a** El Niño Modoki (1994, 2002, and 2004), **b** El Niño (1982, 1987, and 1997) during the data period. **c** Composite of these temperature anomalies for the ''El Niño'' based on 6 largest values of the Nino3.4 index in JJA during the same data period (1982, 1987, 1994, 1997, 2002, and 2004). Anomalies that are not significant at the 80% level are omitted. The SSTAs in the *black boxes* in the panels are used to define the respective indices

posites of SSTA over oceans and surface skin temperature anomalies over land for the three largest El Niño Modoki events (1994, 2002, and 2004; Fig. 2a) with those for the three largest El Niño events (1982, 1987 and 1997; Fig. 2b). These cases are chosen based on magnitude of the two indices in the summers during the data period (Ashok et al. 2007; also shown later in Fig. 4).

In the tropical Pacific there is a tripole structure of the SSTA in El Niño Modoki (Fig. 2a) while a dipole structure in El Niño (Fig. 2b). Associated with those two tropical phenomena in the equatorial Pacific, the SSTA in other oceanic regions also show markedly different patterns. For example, the SSTA in the extratropical North Pacific has a large-scale warm SSTA during summer of El Niño Modoki (Fig. 2a) while a large-scale cool SSTA during summer of El Niño (Fig. 2b). In the North Atlantic, there are SSTA wave trains for both phenomena in the vast region from the Caribbean Sea, through the western North Atlantic and the Norwegian Sea, to the Arctic Ocean. However, the spatial phases of the wave trains between the two phenomena are *almost opposite* with only slight phase shift in both longitude and latitude.

Different teleconnection patterns related to these two phenomena are also found in surface skin temperature over land (Fig. 2a, b). For example, the western North America from Alaska to California, much of Japan, and the lower reach of the Yangtze River valley in China are warm during El Niño Modoki, while cool or near normal during El Niño. The large warm region from east of the Ural Mountain to the northwestern tip of northeastern China, and the cool region in the Pacific coast of South America found during El Niño Modoki (Fig. 2a) experience *almost opposite* conditions during El Niño (Fig. 2b).

Figure 2c is the composite of the six largest ''El Niño'' summers during the data period based on the JJA Niño3.4 index, which is defined by the mean SSTA averaged over the region (170°–120°W, 5°S–5°N). Figure 2c happens to be the average of Fig. 2a, b. It is obvious that many of the aforementioned significant features outside the tropics, which are *almost opposite* in anomaly sign between Fig. 2a and Fig. 2b, are not found in Fig. 2c. The comparison among the three panels in Fig. 2 clearly shows that the ''El Niño'' defined based on the Niño3.4 index presents only the residual signals between two very different phenomena quantified by the EMI and the Niño3 index, respectively; the Niño3.4 index mixes up the El Niño Modoki and the El Niño.

The differences in rainfall anomaly associated with the two phenomena in some Pacific rim countries are also apparent. As example, we compare them for China, Japan, and the USA based on in-situ data in Fig. 3. Figure 3a–c gives the *normal* rainfall amount in the three countries. Figure 3d–i compares the composite rainfall *anomaly percent to normal* in the three countries between the two phenomena. During El Niño Modoki (Fig. 3d–f), the dry areas basically correspond to the aforementioned anomalously warm areas in these countries (Fig. 2a). For example, the warm areas in China (Fig. 2a) are in the lower reach of the Yangtze River valley and the far northern part of northeastern China where the composite rainfall deficits exceed 30% (Fig. 3d). Meanwhile, the cool region in southern China experiences rainfall excess; in some areas

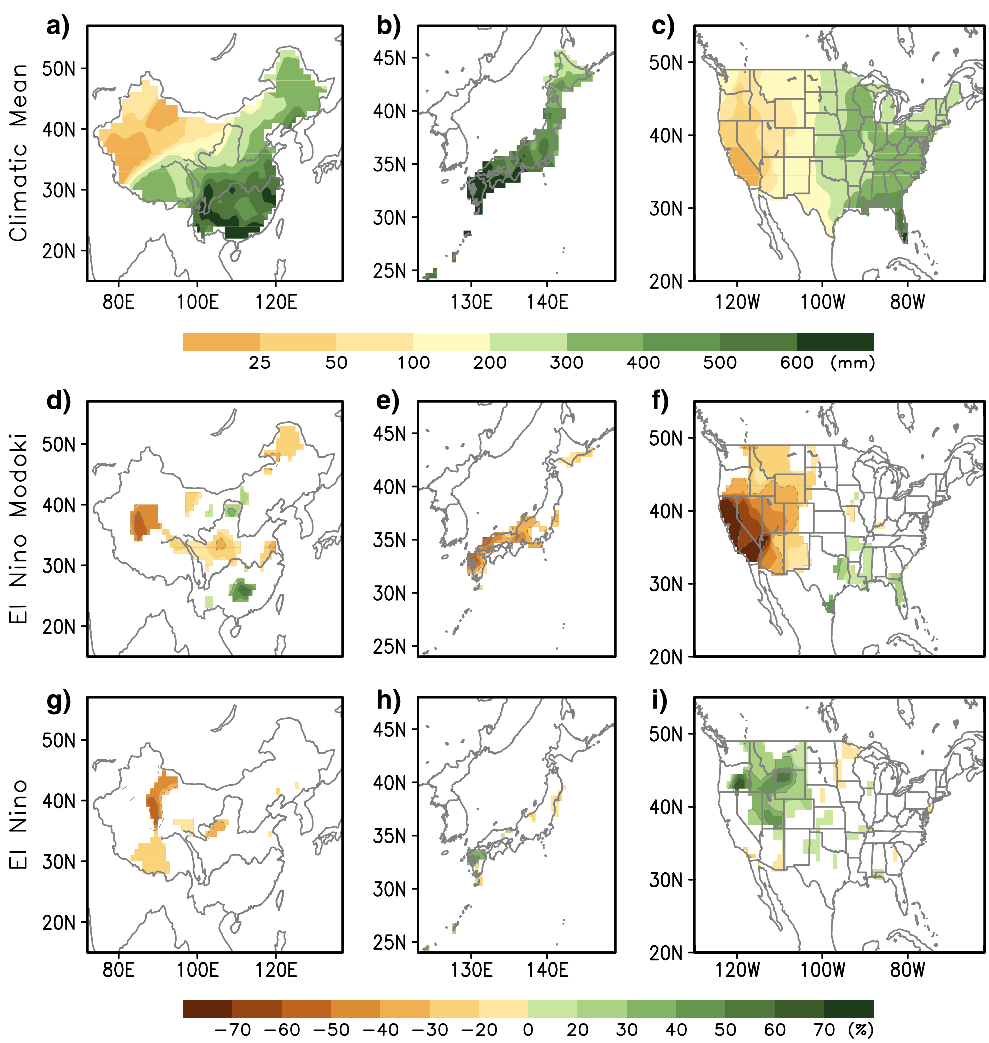

Fig. 3 Climatological (normal) rainfall in **a** China, **b** Japan, and **c** the USA for the summers of 1979–2005. Composite summer rainfall *anomaly percent to normal* (%) for the three largest El Niño Modoki events is shown in **d** China, **e** Japan, and **f** the USA, and that for the three largest El Niño events in **g** China, **h** Japan, and **i** the USA. The values that are not significant at the 80% level are omitted

the excess surpasses as much as 70%. In Japan (Fig. 3e), the significantly warm dry areas are between 35°N and 37°N, as well as in southeastern Hokkaido. The largest rainfall deficits appear in the western part of Japan (the Japan Sea side of Kyushu, western Chugoku, and the Kinki area), where the composite rainfall deficits reach or exceed 40%. These dry areas in China and Japan during El Niño Modoki (Fig. 3d–e) may experience wet or near normal conditions during El Niño (Fig. 3g–h).

The droughts in the western USA during these El Niño Modoki summers (Fig. 3f) are severe. The composite rainfall deficits in some areas of the West surpass 70% while the land skin temperature is warm (Fig. 2a). Meanwhile, the southern and southeastern states are wet due to frequent visits of tropical storms. During El Niño summers (Fig. 3i), most regions of the West receive excess rainfall, except for the southwestern states being nearly normal or slightly dry. The rainfall excess in some areas from southeastern Oregon to northwestern Wyoming, as well as southern Utah is as large as 50% and the areas are relatively cool. The composite rainfall anomaly pattern for El Niño (Fig. 3i) is similar to those in earlier studies with various degrees (e.g., Ropelewski and Halpert 1986, 1996; Higgins et al. 1999; Rajagopalan et al. 2000; Seager et al. 2005). It is apparent that the warm temperature during El Niño Modoki (Fig. 2a) exacerbates the droughts in the areas with large rainfall deficits in these countries.

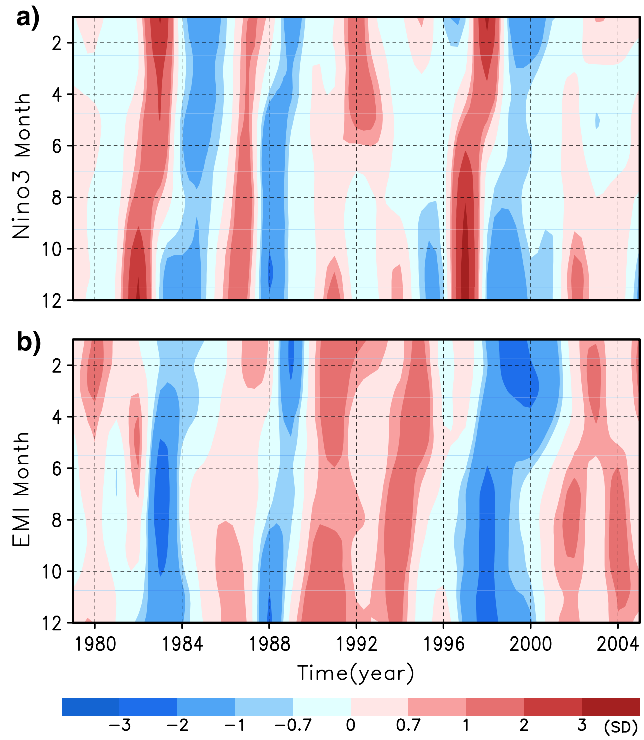

Fig. 4 Normalized monthly time series of **a** Niño and **b** EMI for the period from Jan 1979 through Dec 2005 in the year-month domain. Each month in the ordinate represents a 3-month running mean. The standard deviations for the monthly Niño3 and EMI during the period are 0.887 and 0.503°C, respectively. The indices for the JJA of 1979–2005 are used for the partial correlation and partial regression analyses shown in later figures

3.2 Temporal features and seasonality

We further study the El Niño Modoki phenomenon by comparing the temporal features of the EMI with those of the Niño3. Figure 4 presents the normalized Niño3 and EMI time series in a year–month domain to show whether an index is mainly phase-locked to the seasonal cycle. Figure 5 presents the wavelet coefficients of the two normalized monthly indices to show their dominant timescales.

In general, El Niño events during the data period (Fig. 4a) intensify in late summer to early fall, peak in winter, and decay in the following spring. This feature of phase-locking with the seasonal cycle has been widely studied (e.g., Thompson and Battisti 2000; An and Wang 2001; Tozuka and Yamagata 2003; Luo et al. 2005). As shown in Fig. 5a, the interannual variability of the Niño3 dominates over the decadal variability, which is consistent with earlier studies (Zhang et al. 1997; Diaz et al. 2001; Wang and An 2002; Rogers et al. 2004).

The EMI (Fig. 4b) shows less clear phase-locking with the seasonal cycle compared with the Niño3. In some events, such as in 1994–1995, 2002–2003 and 2004–2005, the EMI values in both late summer and late winter are positively large. During the data period, the positive values of the EMI seem to be *clustered* in three time sections: (1) the early 1980s, (2) the first half of the 1990s, and (3) since 2002. There is also an isolated positive EMI in 1986. The EMI during the data period exhibits large decadal variability (Fig. 5b). Figures 4b and 5b indicate that, on the decadal timescale, the three time sections with clustered positive EMI correspond well to the three positive phases of the EMI, while the isolated event in 1986 is in a negative phase. Based on the criterion to define an El Niño Modoki event using the EMI index (>0.7 standard deviation by Ashok et al. 2007), the positive EMI values in the early 1980s are not qualified as ''events''.

The difference in seasonality between El Niño Modoki and El Niño can also be compared by their related zonal winds over the eastern tropical Pacific. Since the zonal SST gradients in the eastern equatorial Pacific are *opposite* between the two phenomena, the low-level convergence area in El Niño Modoki is expected to be west of that in El Niño. As a result, in the eastern tropical Pacific, the zonal wind direction is mainly opposite between El Niño Modoki and El Niño events. Such a difference at 120°W is shown in Fig. 6 as an example. The zonal wind direction in El Niño Modoki (Fig. 6a) is *opposite* to that in El Niño

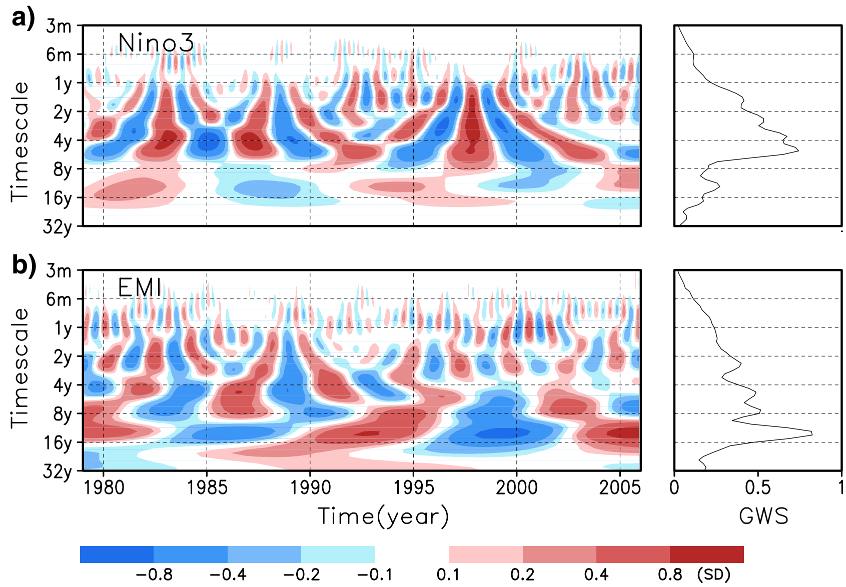

Fig. 5 Morlet wavelet real coefficients (*left panels*) and global wavelet spectra (*right*) of the normalized 3-month running mean time series in Fig. 4 for **a** Niño3 and **b** EMI

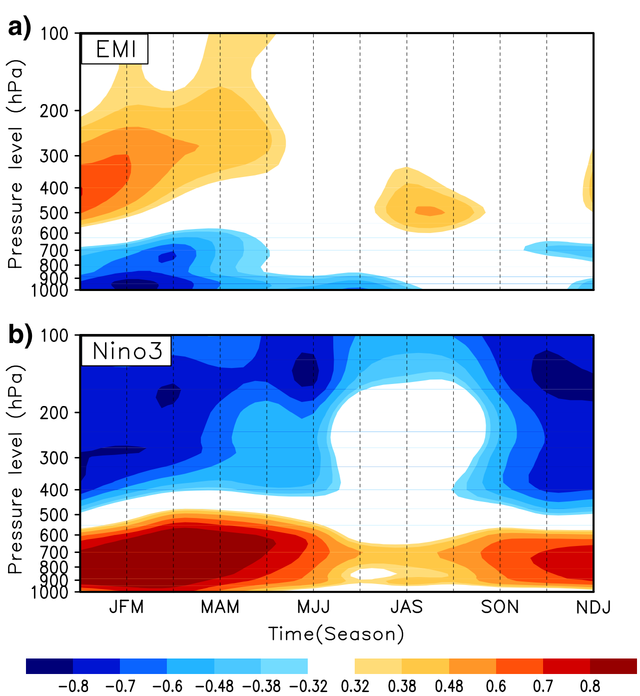

Fig. 6 Partial correlation between the 3-month running mean zonal wind anomalies averaged over (120°W, 10°S–10°N) and the 3-month running mean of each of the two indices, **a** EMI and **b** Niño3, at the pressure levels from 1,000–100 hPa. The correlation coefficients that are not significant at the 90% level are omitted

(Fig. 6b) at most levels almost through the whole ''event year''. For El Niño Modoki, the maximum is found from late winter through early spring. Interestingly, a secondary westerly anomaly center appears near 500 hPa in late summer, showing a more complicated seasonality. This is consistent with the temporal feature of the EMI time series (Fig. 4b). The El Niño related wind anomaly field shows a strong annual signal during the event year, which is also consistent with the temporal feature of the Niño3 time series (Fig. 4a).

In what follows, we endeavor to find possible links between boreal summer dry/wet conditions in some Pacific rim countries during El Niño Modoki, by tracing the teleconnection paths emanating from the equatorial Pacific through anomalous atmospheric circulations. Such anomalous atmospheric circulations are shown to be different from those related to El Niño.

4 Upper-level and vertical atmospheric circulations

4.1 200 hPa

It is well known that the velocity potential at 200 hPa contains information concerning the overall intensity of the tropical circulations and reflects low-level convergence and divergence (e.g., Tanaka et al. 2004). Figure 7 shows upper-level velocity potential and divergent winds related to each of El Niño Modoki and El Niño, which indicate how upper-level air flows from the mass sources to sinks.

For El Niño Modoki (Fig. 7a), the main upper-level mass source (divergence center) is over the central Pacific between 10°S and 10°N near the Dateline where SSTA is positive (Fig. 2a). The main upper-level mass sink (convergence center) is over the southeastern Indonesia. A secondary upper-level mass sink is found over the far eastern equatorial Pacific and southern Mexico. The tripole structure of the upper-level divergence/convergence over the tropical Pacific corresponds well to the tripole SSTA distribution in this region (Fig. 2a).

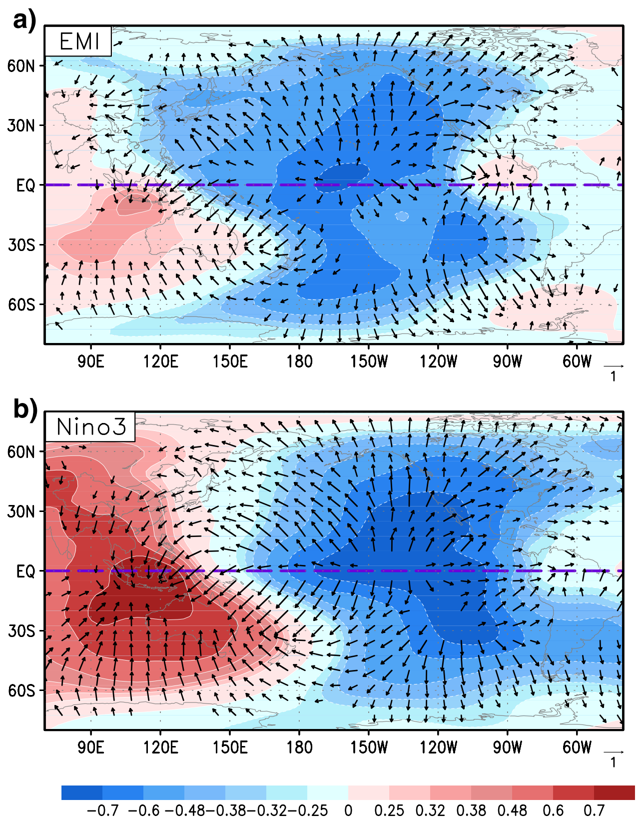

Fig. 7 Partial correlation patterns of the 200 hPa divergent winds (*arrow*) and velocity potential anomalies (*shading*) with **a** EMI and **b** Niño3 in the domain of (70°E–40°W, 80°S–80°N). The wind vectors with correlation coefficients of either zonal or meridional component that are not significant at the 90% level are omitted

Over the western North Pacific, the upper-level divergence/convergence related to El Niño Modoki has important impacts on the climate in Japan and eastern China through at least *two* paths. The first path reflects a *direct* influence from the central equatorial warm Pacific. The anomalous southeasterly divergent winds from the main mass source directly converge over Japan, East China Sea, and the western North Pacific to the north of the Philippines.

The second path is an *indirect* and more complicated one. Normally, the heat source to drive a summer monsoon in the western North Pacific summer monsoon region is dynamically related to the upper-level divergent circulation centered near the Philippines over the warm pool (Krishnamurti 1971; also see Fig. 1a, b). During El Niño Modoki, the area with maximum anomalous convection over the warm pool, reflected by the upper-level anomalous mass source, shifts eastward in the tropical Pacific (Fig. 7a) compared with the climatological mean (Fig. 1a, b). A part of the southeasterly flow from the main mass source turns southwestward and converges to the main mass sink, which causes weak upper-level divergence over the Philippine Sea. Such a mass flow has a large influence on the western North Pacific summer monsoon and the East Asian summer monsoon. The descent over Indonesia, as a part of the anomalous Walker Circulation, suppresses the convection there and causes low-level divergent flow. The part of the northward divergent flow excites a secondary anomalous regional meridional circulation with ascent to its north (figure not shown). The aforementioned upper-level weak anomalous divergence zone over the Philippine Sea enhances the low-level convection over the region, which in turn enhances the western North Pacific summer monsoon. The latter weakens the East Asian summer monsoon through another secondary regional meridional circulation with descent to further north. The influences of El Niño Modoki on the climate in East Asia through these monsoons will be discussed in more detail in Sect. 5.

Strong anomalous northeasterly divergent winds from the main mass source flow toward southern Indonesia as well as northern and eastern Australia forming an anomalous upper-level convergence zone (Fig. 7a). The latter forces strong descending motion and anomalous low-level divergence as well as below-normal rainfall there.

For El Niño (Fig. 7b), the main upper-level mass source is located over the eastern tropical Pacific. The main upper-level mass sink centered over Indonesia and northwestern Australia (Fig. 7b) is more intensive than that for the case of El Niño Modoki (Fig. 7a). Over the western North Pacific, there is also an upper-level convergence band, which is located southeast of its counterpart in El Niño Modoki (Fig. 7a), i.e., away from Japan. This displacement implies that the main descent in that region is also displaced southeastward, with less descent over Japan compared with the situation in El Niño Modoki. The anomalous northeasterly divergent winds from the main mass source to the main mass sink also converge over a northwest–southeast oriented zone, which is stronger and displaced slightly eastward than its counterpart in El Niño Modoki (Fig. 7a). As expected, the maximum descent over this region would also shift eastward compared to that in El Niño Modoki.

Similarly, in the central-eastern Pacific during El Niño Modoki (Fig. 7a), the combination of the anomalous upper-level divergence over the central tropical Pacific and the convergence over the eastern tropical Pacific results in strong descending motion over the eastern tropical Pacific and Mexico as a part of Walker Circulation. The secondary divergence center over the eastern South Pacific near (120°W, 30°S) and the convergence over the southern tip of South America, combined with the convergence center over the eastern tropical Pacific reflects strong regional meridional circulations (figure not shown) and tropical–extratropical interaction in the eastern South Pacific and adjacent South America. It should be noted that, although the two positive velocity potential centers shown by linear correlation are not significant even at the 80% level, the convergence indicated by the divergent wind related to these centers are significant at the 95% level. These results are consistent dynamically.

During El Niño (Fig. 7b), over the eastern Pacific, there is negative velocity potential with no apparent upper-level convergence over ocean and very weak convergence over the tropical South America. This situation implies that there must be different vertical flows in the tropical South America between the two phenomena. Moreover, since the upper-level divergence in the eastern tropical Pacific is strong, so that the areas with negative velocity potential extend northeastward and southeastward to pass over North and South Americas. As a result, during El Niño summer, the west coastal areas in both Americas are more likely to have updraft and associated rainfall, which will be further compared in Sect. 5.

4.2 Walker Circulations

The Walker Circulation over the tropical Pacific during El Niño Modoki (Fig. 8a) exhibits a clear two-cell pattern in the troposphere. The joint ascending branches cover a broad range in the central tropical Pacific between 135°E and 125°W, associated with anomalous wetness and the main upper-level mass source near 200 hPa. The descending branches of the two cells are over the western and eastern tropical Pacific, corresponding to SSTA distribution (Fig. 2a) and anomalous upper-level mass sinks (Fig. 7a). The strong descending motion between 100° and 130°E and the low-level divergent flows of the western cell are in the region where the normal Inter-Tropical Convergence Zone (ITCZ) and the South Pacific Convergence Zone (SPCZ) may meet (Fig. 1b; also Waliser and Gautier 1993). Therefore, the normal convection there is suppressed during El Niño Modoki. Both descending branches correspond to dry conditions.

The Walker Circulation related to El Niño (Fig. 8b) shows a two-cell structure between 90°E and 60°W. However, there is only one-and-a-half cell over the tropical

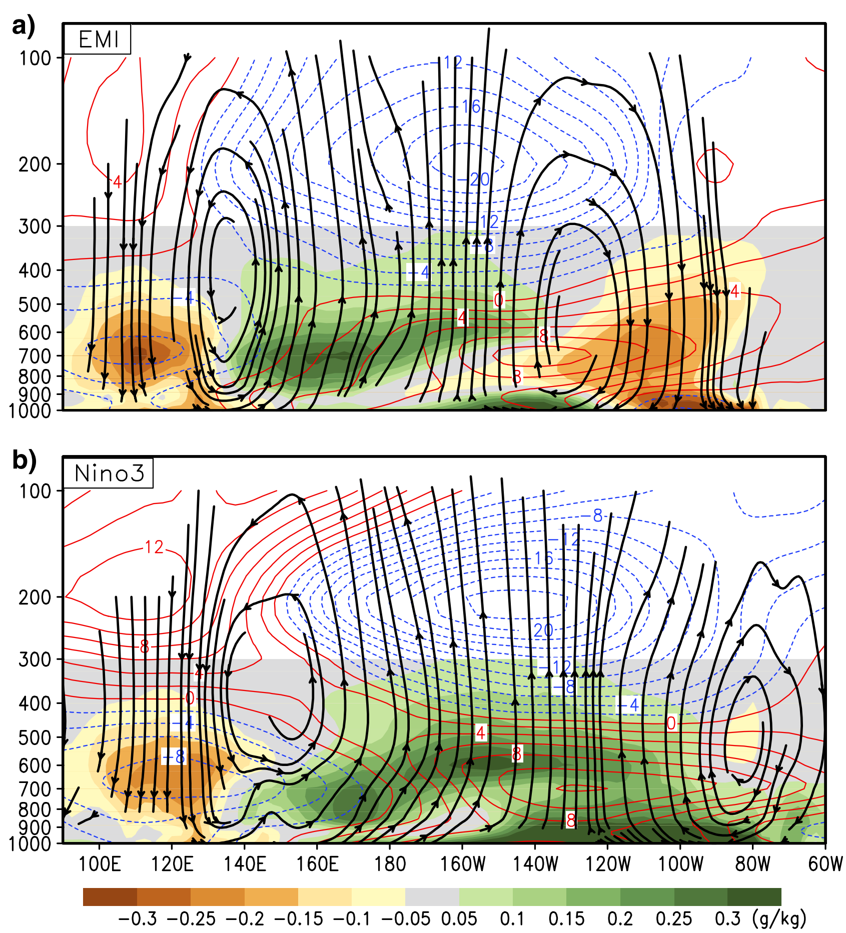

Fig. 8 Anomalous Walker Circulations between 90°E and 60°W based on partial regression between the anomalous velocities averaged over (10°S–10°N) and one of the two indices **a** EMI and **b** Niño3. The anomalous vertical velocity at the pressure levels has been multiplied by a factor of –50 to give a better view. The regressed specific humidity is *shaded*. The contours are for regressed velocity potential (interval: 2×10^5 m^2 s^{-1}). The units labeled in all the regression patterns here and for the remaining figures are actually the units per standard deviation of the index being regressed. The standard deviations for EMI and Niño3 in JJA are 0.495 and 0.749°C, respectively

Pacific. Most of the tropical Pacific is covered by a wide ascending branch, spanning over 150°E–85°W, flanked by the descending branches west of 140°E and east of 80°W. The western and eastern boundaries of the ascending region are positioned about 15 and 40°, respectively, in longitude to east of those of the Walker Circulation in El Niño Modoki (Fig. 8a, b). The descent over Indonesia in El Niño (Fig. 8b) is stronger than that in El Niño Modoki (Fig. 8a). On the contrary, the east cell in El Niño is much weaker than that of the El Niño Modoki, indicated by its shallow overturning. Although much of Indonesia is in a descending branch during both phenomena, stronger subsidence is more likely to appear in its western (eastern) region during El Niño Modoki (El Niño).

5 Mid- and low-tropospheric circulations and related dry/wet conditions

5.1 500 hPa gph anomaly

The 500 hPa gph anomaly field is often used to study large-scale circulations in the mid-troposphere, which is closely related to the low-level wave activity in the mid-latitudes (e.g., Bluestein 1993). The latter in turn relates to regional moisture and rainfall distribution (e.g., Shukla and Wallace 1983). Different wave patterns in the 500 hPa gph anomaly fields presented here may be considered as linear response of the mid-latitude wave activity to different tropical SSTA forcing in the summer season during the two phenomena.

For El Niño Modoki (Fig. 9a), there are two wave trains crossing the mid- (~30°–45°N) and high- (~55°–75°N) latitude North Pacific basin. In the western North Pacific, there is an anomalous high over much of Japan and anomalous lows to its north and southwest. The anomalous high and the anomalous low to its southwest form a positive phase of the Pacific-Japan pattern (Nitta 1987). The pair implies that the western North Pacific subtropical high has intensified and advanced northwestward over (135°E, 30°N) from its climatological mean over (160°E, 25°N; Fig. 1b), and that the areas from the South China Sea to the Philippines experience frequent cyclonic activity. The anomalous low to the north of Japan implies that the Okhotsk high is unusually weak. The position and the intensity of these anomaly centers have great impacts on the climate of East Asia through low-level circulations, such as the monsoons in this region (Wang and Yasunari 1994; Chang et al. 2000; Yang and Sun 2003; Wakabayashi and Kawamura 2004; Weng et al. 2004).

In the eastern North Pacific and North America, there is a pronounced positive phase of a summer Pacific-North American (PNA) pattern[10]. The location and intensity of each component of the summer PNA pattern during El Niño Modoki has great impacts on the climate condition in Mexico and North America, especially on the climate in the USA. The anomalous low over the central-eastern North Pacific implies that the Aleutian low is expanded southeastward. As a result, the normal trough over the west coast of North America at 500 hPa (Fig. 1b) shifts westward to be off the west coast (Fig. 9a).

The anomalous high over the west coast of North America is a combination of the anomalous highs in both subtropical and extratropical wave trains in that region. The northern one corresponds to the warm anomalies in the eastern tip of Russia, Alaska, and western Canada (Fig. 2a). The southern one implies that the normal ridge over the Midwest of the USA (Fig. 1b) shifts westward to be over the west coast of the USA. Such a shift is influenced by the enhancement of its upstream anomalous low. It, in turn, enhances the downstream trough over the east coast of North America (Fig. 1b) and ''pulls'' it westward, manifested by an intense anomalous low right over the central North America (Fig. 9a).

For El Niño (Fig. 9b), there is no clear PNA-like pattern in the eastern Pacific and North America, which is apparent in El Niño Modoki (Fig. 9a). Instead, there is a zonally oriented anomalous low band across the mid-latitude North Pacific with two anomalous low centers: the stronger one is to the east of Japan and the weaker one is over the west coast of the USA. The western North Pacific subtropical high is retreated southeastward to south of 30°N. Both Japan and the western USA are under the influence of positive (negative) 500 hPa gph anomalies during El Niño Modoki (El Niño).

In the South Pacific where it is austral winter during JJA, there are basin-wide anomalous lows in the mid-latitude and anomalous highs in the high-latitude in both Fig. 9a, b. However, the anomalies over Australia and South America are very different between the two phenomena. The differences in location and intensity of these anomalous highs and lows between the two phenomena are

[10] The PNA pattern is most pronounced in boreal winter, but very weak in boreal summer (e.g., Wallace and Gutzler 1981). Based on NOAA's map for PNA patterns at 500 hPa (http://www.cpc.ncep.noaa.gov/data/teledoc/pna_map.shtml), the positive phase of July PNA features above-average heights to the west of Hawaii and the southeastern USA and below-average heights over the southern Aleutian Islands and the eastern Canada. The above-average heights over the western North America that are apparent in the positive phase of PNA in other seasons are hardly discerned in July. It is this component of the summer PNA that exerts great impact on the climate in the western USA during El Niño Modoki. Note that the strength and location of the PNA components have a seasonal dependence due to various forcings including SSTA in the tropical Pacific (Leathers and Palecki 1992).

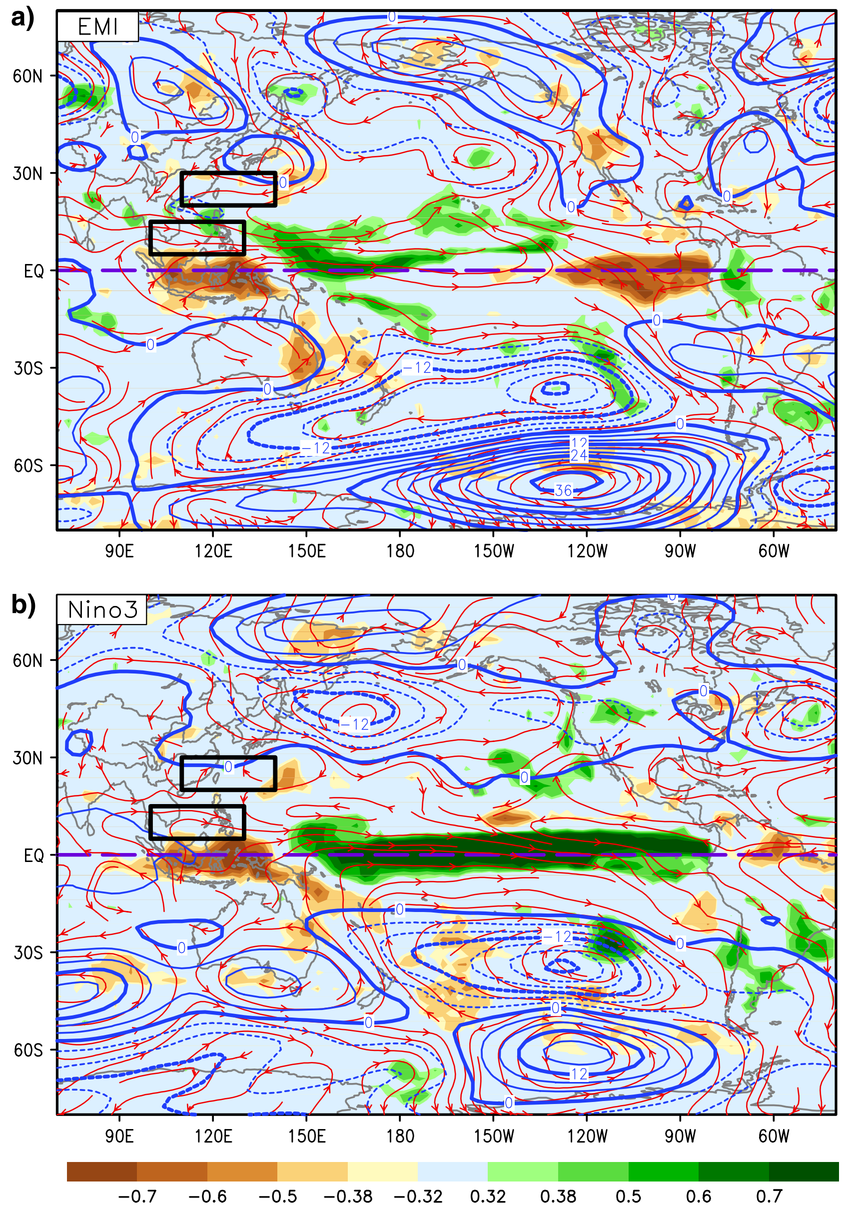

Fig. 9 Partial regression anomaly patterns of the 500 hPa geopotential height (*blue contours*; unit: *m*), 850 hPa wind (*red streamlines*), and the partial correlation pattern of GPCP precipitation rate anomalies (*shading*) with **a** EMI and **b** Nino3. The precipitation correlation coefficients that are not significant at the 90% level are omitted. The 850 hPa zonal wind anomalies in the two black boxes are used to calculate the WNPSMI defined by Wang and Fan (1999)

well related to the upper-level velocity potential fields shown earlier. They also imply different low-level circulation and related rainfall patterns between El Niño Modoki and El Niño events that will be shown next.

5.2 850 hPa wind and related rainfall

The 850 hPa wind anomalies presented by streamlines are consistent with their respective 500 hPa gph anomaly fields in the mid- and high-latitudes for both phenomena. Since there is little signal at 500 hPa gph anomaly field in the tropics, the 850 hPa wind anomalies in the tropics are important to show the difference in impacts of the two phenomena on the climate in the tropics and beyond.

For El Niño Modoki (Fig. 9a), there are westerly (easterly) wind anomalies over the western (eastern) tropical Pacific, implying that the local climatological trade wind shown in Fig. 1b is weakened (enhanced). The westerly wind anomalies meet the easterly wind anomalies near 150°–130°W. The central-western (eastern) equatorial Pacific is wetter (drier) than normal. Moreover, the westerly wind anomalies from the western tropical Pacific seem to divert into three branches near 160°E. From there one branch is maintained eastward along the equator, while the other two turn northeastward and southeastward in the North and South Pacific, respectively. Correspondingly, there are three branches of the wet zones in the central tropical Pacific. The two branches that are located on and to the north of the equator imply a northward expansion of the ITCZ. The wet branch to the south of the equator implies an enhanced and slightly southward expanded SPCZ. Thus, the northeastward and southeastward wind anomalies transport the anomalous moisture from the central-western tropical Pacific to the central subtropical North and South Pacific Oceans, respectively. However, for El Niño (Fig. 9b), the westerly wind anomalies from the western tropical Pacific cross the equatorial Pacific basin all the way to the coast of South America. The anomalous westerlies concentrate on the equator and nearby. Thus, both ITCZ and SPCZ seem to shift equatorward and merge into a single broad wet band, which extends from the west of the Dateline to the west coast of South America. The moisture transport from the tropics to the subtropics mainly occurs in the eastern Pacific in both hemispheres.

The differences in the low-level circulation and the dry/wet distributions in the tropical Pacific between the two phenomena are well related to the differences in the upper- and mid-level atmospheric circulations, as well as the Walker Circulations (Fig. 8) and regional meridional circulations (figures not shown). For example, much of Indonesia suffers dry conditions during both phenomena, with the driest area being more likely in its western (eastern) part in El Niño Modoki (El Niño); it is consistent with the location of the strong descending motion in their respective Walker Circulations. In the eastern tropical Pacific, because of the opposite anomalous zonal and meridional SSTA gradients between the two phenomena, it is expected that the low-level convergence and rainfall anomaly in that region would be very different (Lindzen and Nigam 1987). Due to the dynamical forcing of the dry (wet) downdraft (updraft) in El Niño Modoki (El Niño) in the eastern tropical Pacific, some areas in the adjacent tropical South America east of the Andes experience opposite rainfall anomalies from those in the neighboring eastern equatorial Pacific.

In the extratropics in both hemispheres, the differences in wind anomaly patterns between the two phenomena are also obvious. For example, in the western North Pacific, there is a large difference in the western North Pacific summer monsoon and the East Asian summer monsoon between the two phenomena. For better comparison, we quantify such a difference by using the western North Pacific monsoon index (WNPMI) defined by Wang and Fan (1999), which is the difference of 850 hPa westerlies between a southern region (100°–130°E, 5°–15°N) and a northern region (110°–140°E, 20°–30°N); the areas are marked in Fig. 9. The mean WNPMI averaged for the three largest El Niño Modoki (El Niño) summers during our data period is 2.53 (–1.03). The largest positive value of the WNPMI during the data period is 3.18, which appeared in the summer of 2004—during the most recent El Niño Modoki event. The difference in the mean WNPMI between the two composite phenomena implies that the western North Pacific summer monsoon in El Niño Modoki (El Niño) is more likely to be stronger (weaker) than normal. Since the phases of the western North Pacific summer monsoon and the East Asian summer monsoon are basically opposite on interannual timescale (Wang et al. 2001), the East Asian summer monsoon in El Niño Modoki (El Niño) is more likely to be weaker (stronger) than normal, which is also closely related to the position and intensity of the 500 hPa Pacific-Japan pattern there. Thus, in El Niño Modoki, the Philippines and the southern coastal China are more likely to be wet due to enhanced western North Pacific summer monsoon, while Japan and the Yangtze River valley in China are more likely to suffer from drought due to weakened East Asian summer monsoon. The rainfall anomalies in these regions during El Niño (Fig. 9b) are very different (e.g., Huang and Wu 1989; Weng et al. 1999; Lau and Weng 2001). The differences in rainfall anomaly patterns are further confirmed by the partial correlation between the in-situ data in China/Japan and the EMI and Niño3 index as shown in Fig. 10.

Most of previous studies did not recognize the role of El Niño Modoki events when looking at canonical ''El Niño impact'' on the western North Pacific summer monsoon. For example, Wang et al. (2001) hypothesized that a weak (strong) western North Pacific summer monsoon tends to occur in the summer *after* the mature phase of warm (cold) ENSO. It is interesting to find that the largest positive WNPMI during the period of 1948–1997 calculated by Wang et al. (2001) occurred in the summer of 1994; it is exactly during an El Niño Modoki event. All the three largest El Niño Modoki events during our data period did not occur in the summer ''after'' the mature phase of a cold ENSO. This fact further elucidates that the intensities of the western North Pacific summer monsoon and the East Asian summer monsoon do not have a simple relation with the phase of the warm-cold ENSO cycle (Chou et al. 2003). It further shows that El Niño Modoki is not necessarily one stage of the ENSO cycle, so that the influence of El Niño Modoki on these monsoons should not be mixed up with that of El Niño.

The difference in the low-level wind anomaly in the eastern North Pacific between the two phenomena is also apparent. For example, for El Niño Modoki (Fig. 9a), there are southwesterly wind anomalies over the eastern North Pacific off North America between the 500 hPa low and high anomalies, and there are northerly dry wind anomalies over the western USA. These wind anomalies cause wetness over the eastern Pacific and dryness in the western USA and Baja California (Mexico). The dryness extends to the northern Great Plains, the western Canada and the central Alaska (Fig. 9a). For El Niño (Fig. 9b), the southwesterly wind anomalies over the eastern North Pacific extend eastward and enter the western USA along the southern flank of the 500 hPa low band near 30°N. The low-level wind anomalies bring more moisture to this region, opposite to the El Niño Modoki case.

In the eastern USA, the rainfall anomaly is mainly influenced by the anomalous moisture transport from the Atlantic Ocean and the Gulf of Mexico, not from the Pacific Ocean. However, as shown in Fig. 2a, b, the SST anomaly patterns in the North Atlantic related to the two phenomena are basically opposite. It shows that the atmospheric circulations and moisture transport over there could also be very different under different influences of the two phenomena. In El Niño Modoki (Fig. 9a), the easterly wind anomaly on the southern flank of the enhanced Bermuda high at 500 hPa and the anticyclonic wind anomaly at 850 hPa off the east coast of the USA favor bringing in tropical storm and abundant moisture to that area. This is not the case in El Niño (Fig. 9b) when there is an anomalous low at 500 hPa off the east coast of the USA, because the westerly wind anomalies do not favor moisture transport from Atlantic Ocean to the southeastern states (e.g., Gray 1984). The detailed difference in rainfall anomaly in the USA, especially in the western and southeastern states, between the two phenomena is more apparent by using the 102-divisional rainfall data as shown in Fig. 10c, f.

In the South Pacific, some remote responses to El Niño have been studied (e.g., Andrade and Sellers 1988; Grimm et al. 2000; Zhou and Lau 2001; Vera et al. 2004). In the western South America, the main difference appears in northern Chile because it is in the northern flank of the anomalous eastern South Pacific high in El Niño Modoki while under anomalous low in El Niño. Thus, the area is very likely to be dry in El Niño Modoki while wet in El Niño. The rainfall anomaly distribution in Australia and its adjacent region is very sensitive to the displacement of the SPCZ and its adjacent dry zone to its southwest. As a result of such a displacement, the dryness in the eastern Australia and northern New Zealand may be more severe in El Niño Modoki than that in El Niño. It should be noted that the rainfall anomaly in Australia and its adjacent region is also under large influence from the mid-latitude systems during boreal summer, although some of the anomalous mid-latitude systems may be generated by the tropical SSTA. Thus, the rainfall anomaly there is a combined influence of the tropical–extratropical interaction.

6 Discussions and concluding remarks

Using recent 27-year multiple observational data sets, we have shown the existence of the El Niño Modoki as a distinguished phenomenon in the tropical Pacific from the canonical El Niño. We have also found possible links between boreal summer dry/wet conditions in the Pacific rim and the El Niño Modoki, by tracing the teleconnection paths emanating from the equatorial Pacific through anomalous atmospheric circulations, which are different from those related to El Niño.

Whether an El Niño Modoki event is strong or weak may introduce some differences in the characteristics of its teleconnection patterns. If an El Niño Modoki event is weak, other major factors such as the Arctic Oscillation that influences the rainfall in the northern Pacific rim

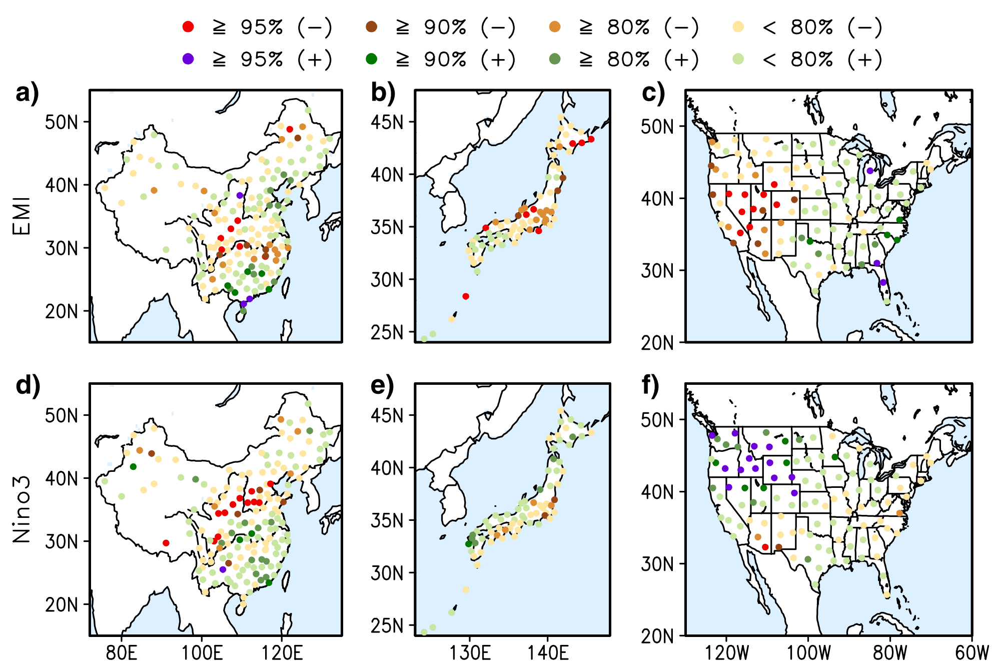

Fig. 10 Partial correlations between in-situ JJA rainfall anomalies in China, Japan, and the USA with the EMI (*a*, *b*, *c*) and those with the Nino3 index (*d*, *e*, *f*), respectively. The correlations that are not significant at the 80% level are also given with the *lightest colored dots* for reference

countries may play more important roles than a weak El Niño Modoki does from the tropics. That is one reason why we have chosen the three largest El Niño Modoki events and three largest El Niño events during the data period for the composites (Figs. 2, 3) to elucidate the most characteristic features of the two different phenomena.

Moreover, since the three El Niño Modoki events and three El Niño events are well separated in time, no one event of one kind of phenomenon can be considered as an evolving phase of an event of another kind on interannual timescale. Therefore, the signals of one kind of phenomenon are not smeared by another. The teleconnection patterns shown by partial correlation/regression analyses further suggest that the El Niño Modoki and El Niño are two different phenomena in both space and time.

The SSTA in the extratropical North Pacific is important to the rainfall anomaly in the western and central USA (e.g., Ting and Wang 1997). Recent model experiments have suggested that the persistent tropical Pacific SST variations are very likely the ultimate driver of the persistent drought and precipitation events over the Plains and Southwest of the USA. This is because the SST anomalies outside the tropical Pacific may themselves be initially forced as a remote response to SST variability in the tropical Pacific (e.g., Seager et al. 2005). It is possible that different extratropical influences on the rainfall anomaly in these regions may actually be related to different tropical origins between El Niño Modoki and El Niño events.

The three El Niño Modoki events for the composites are in positive phases on the decadal timescale. Since the SSTA in the extratropical North Pacific is also influenced by, say, the decadal Arctic Oscillation, the response of the extratropical SSTA to the tropical SSTA distribution may be different in negative decadal phase (e.g., the 1986 event). Therefore, caution must be made when applying the composite results obtained here to other time section in negative phase on decadal timescale of El Niño Modoki. The aforementioned relationships should be further studied by numerical experiments.

Some model simulations (e.g., Lau et al. 2005) indicate that the rainfall and surface temperature anomalies in the North American sector tend to have an increased frequency of droughts and heat waves during the summer season after warm ENSO events. However, the observational fact is that there were no major El Niño events after the 1997–1998 one, yet there was a large-scale *persistent* drought in the western USA from the early through mid-2000s. This persistent extreme climate condition could be related to El Niño Modoki in a positive phase on the decadal timescale during the same period (Fig. 5a). Because of the EMI related 850 hPa wind anomalies and poleward displacement of the ITCZ in the central Pacific, the influence of El Niño Modoki with larger decadal background on the climate outside tropics may have larger extent in latitude than that in El Niño. Thus, El Niño Modoki may have a larger tropical–extratropical interaction than El Niño on the decadal timescale that have important influence on persistent climate extremes in North America (e.g., Cayan et al. 1998; Barlow et al. 2001; Hu and Feng 2001; Seager et al. 2005).

It is well known that El Niño events change the likelihood of particular climate teleconnection patterns around the world, but the outcomes of each event are never exactly the same. This is because that the factors such as the change in local Hadley circulation (Slingo and Annamalai 2000) and the location of the warmest SST anomalies in the tropical Pacific (Kumar et al. 2006) are also important when we consider regional climate impact exerted by El Niño. It is also true that no two El Niño Modoki phenomena and their teleconnection patterns are exactly the same. Since the EMI is defined by three area-averaged SSTA in the tropical Pacific, two El Niño Modoki phenomena with the same magnitude of the EMI may have different SSTA patterns in the tropical Pacific. As long as the two side regions are cool enough compared to the central equatorial Pacific, the El Niño Modoki phenomenon may be established. It is the combination of the opposite zonal SST gradients between the western and eastern tropical Pacific that plays a crucial role in causing the anomalous two-cell Walker Circulation in the tropical Pacific: the *heart* of the El Niño Modoki phenomenon. Due to the two-cell Walker Circulation in the tropical Pacific, the characteristic teleconnection paths of the influence from the SSTA in the tropical Pacific during El Niño Modoki to regional climate in the Pacific rim can be distinguished from those during El Niño. Since regional climate impacts of El Niño Modoki in the Pacific rim countries, e.g., those in East Asia and North America, depend more on the zonal SST gradients in the western and eastern tropical Pacific, respectively, it is desirable to build more sophisticated El Niño Modoki indices in the future to reflect the delicate influence of such a difference in zonal SST gradients on the climate in some specific regions of the Pacific rim.

As we have shown in this work that El Niño, though its importance is of no doubt, is not the only phenomenon in the tropical Pacific that exerts global and regional climate impacts. The linear analyses provided here have shown the importance of the El Niño Modoki phenomenon that excites very different teleconnection patterns from those of the canonical El Niño. Furthermore, the results presented here also cast some doubt on whether the Niño3.4 index should be used to identify the canonical El Niño phenomenon, because this index picks up the warming signal in either eastern or central equatorial Pacific. As a result, the Niño3.4 index related teleconnection patterns represent the mixed-up signals of the two different teleconnection patterns distinguished here. Mixing-up the two different phenomena would not only increase the difficulty in understanding their mechanisms and climate impacts, but also increase the uncertainty in their predictions. The El Niño Modoki phenomenon, which has been overlooked for so long under the shadow of El Niño, deserves more attention from the climate community to better understand its spatial and temporal characteristics as well as its various climate impacts.

Acknowledgments We are thankful to Y. He for the U.S. 102-division rainfall data, to S.-W. Wang and J.-B. Huang for the 160-station rainfall data in China, to R.-C. Zhang, H. Shibata and T. Maeda for their help in processing rainfall data in Japan. We appreciate very much for the constructive comments from three anonymous reviewers. Our special thanks go to P. Delecluse for her encouragement and inspiring remarks. HW also extends her thanks to S. Hakeem, Y.-M. Liu, J.-J. Luo, and D.-P. Shi for various discussions, to Z. Yu for her many critical remarks to improve the manuscript.

References

Adler RF, Huffman GJ, Chang A, Ferraro R, Xie P, Janowiak J, Rudolf B, Schneider U, Curtis S, Bolvin D, Gruber A, Susskind J, Arkin P (2003) The Version 2 Global Precipitation Climatology Project (GPCP) monthly precipitation analysis (1979–present). J Hydrometeor 4:1147–1167

An SI, Wang B (2001) Mechanisms of locking of the El Niño and La Niña nature phases to boreal winter. J Clim 14:2164–2176

Andrade ER, Sellers WD (1988) El Niño and its effect on precipitation in Arizona and western New Mexico. J Climatol 8:403–410

Ashok K, Behera S, Rao AS, Weng HY, Yamagata T (2007) El Niño Modoki and its teleconnection. J Geophys Res (Submitted)

Barlow M, Nigam S, Berbery EH (2001) ENSO, Pacific decadal variability, and US summertime precipitation, drought, and stream flow. J Clim 14:2105–2128

Behera SK, Yamagata T (2003) Influence of the Indian Ocean dipole on the Southern oscillation. J Meteor Soc Jpn 81:169–177

Bjerknes J (1969) Atmospheric teleconnections from the equatorial Pacific. Mon Wea Rev 97:163–172

Bluestein HB (1993) Synoptic-dynamic meteorology in midlatitudes. vol II: Observations and theory of weather systems. Oxford University, New York, p 594

Cayan DR, Dettinger MD, Diaz HF, Graham NE (1998) Decadal variability of precipitation over western North America. J Clim 11:3148–3166

Chan JCL (2000) Tropical cyclone activity over the western North Pacific associated with El Niño and La Niña events. J Clim 13:2960–2972

Chang CP, Zhang Y, Li T (2000) Interannual and interdecadal variations of the East Asian summer monsoon and tropical Pacific SSTs. Part I: roles of the subtropical ridge. J Clim 13:4310–4325

Chia HH, Roplewski CF (2002) The interannual variability in the genesis location of tropical cyclones in the northwest Pacific. J Clim 15:2934–2944

Chou C, Tu JY, Yu JY (2003) Interannual variability of the western North Pacific summer monsoon: differences between ENSO and non-ENSO years. J Clim 16:2275–2287

Coughlan M, Jones DA, Plummer N, Watkins AB, Trewin BC, Dawkins SS (2004) Impacts of the 2002–03 El Niño on Australian climate. In: Plummer N, Flannery M, Mullen C, Trewin B, Watkins A, Wright W, Powell T, Power S (eds) DroughtCom Workshop, improving the communication of climate information, vol II, extended abstracts, 22–23 July 2003, Melbourne, Bureau of Meteorology, Commonwealth of Australia, pp 7–12

Diaz HF, Hoerling MP, Eischeid JK (2001) ENSO variability, teleconnections and climate change. Int J Climatol 21:1845–1862

Ding YH, Chan JCL (2005) The East Asian summer monsoon: an overview. Meteorol Atmos Phys 89:117–142

Gray WM (1984) Atlantic seasonal hurricane frequency. Part I: El Niño and 30 mb quasi-biennial oscillation influences. Mon Wea Rev 112:1649–1668

Grimm AM, Barros VR, Doyle ME (2000) Climate variability in southern South America associated with El Niño and La Nina events. J Clim 13:35–58

Hu Q, Feng S (2001) Variations of teleconnection of ENSO and interannual variation in summer rainfall in the central United States. J Clim 14:2469–2480

Huang R, Wu Y (1989) The influence of ENSO on the summer climate change in China and its mechanisms. Adv Atmos Sci 6:21–32

Higgins RW, Chen Y, Douglas AV (1999) Interannual variability of the North American warm season precipitation regime. J Clim 12:653–679

Kalnay E et al (1996) The NCEP/NCAR 40-year reanalysis project. Bull Am Meteor Soc 77:437–471

Kang IS, Kug JS (2002) El Nino and La Nina SST anomalies: asymmetric characteristics associated with their wind stress anomalies. J Geophys Rea 107(D19):4372. doi:10.1029/2001JD000393

Kim JH, Ho CH, Sui CH (2005) Circulation features associated with the record-breaking typhoon landfall on Japan in 2004. Geophys Res Lett 32:L14713. doi:10.1029/2005GL022494

Krishnamurti TN (1971) Tropical east–west circulations during northern summer. J Atmos Sci 28:1342–1347

Kumar KK, Rajagopalan B, Hoerling M, Bates G, Cane M (2006) Unraveling the mystery of Indian Monsoon failure during El Niño. Science 314:115–119, doi:10.1126/science.1131152

Larkin NK, Harrison DE (2005) On the definition of El Niño and associated seasonal average U.S. weather anomalies. Geophys Res Lett 32:L13705. doi:10.1029/2005GL022738

Lau KM, Weng HY (1995) Climate signal detection using wavelet transform: How to make a time series sing. Bull Amer Meteor Soc 76:2391–2402

Lau KM, Weng HY (2001) Coherent modes of global SST and summer rainfall over China: an assessment of the regional impacts of the 1997–98 El Niño. J Clim 14:1294–1308

Lau NC, Leetmaa A, Nath MJ, Wang HL (2005) Influences of ENSO-induced Indo-Western Pacific SST anomalies on extratropical atmospheric variability during the boreal summer. J Clim 18:2922–2942

Leathers DJ, Palecki MA (1992) The Pacific/North American teleconnection pattern and United States climate. Part II: temporal characteristics and index specification. J Clim 5:707–716

Lindzen RS, Nigam S (1987) On the role of sea surface temperature gradients in forcing low-level winds and convergence in the tropics. J Atmos Sci 44:2418–2436

Luo JJ, Masson S, Behera S, Shingu S, Yamagata T (2005) Seasonal climate predictability in a coupled OAGCM using a different approach for ensemble forecasts. J Clim 18:4474–4497

McPhaden MJ (2004) Evolution of the 2002/03 El Niño. Bull Am Meteor Soc 85:677–695

Neelin JD, Battisti DS, Hirst AC, Jin FF, Wakata Y, Yamagata T, Zebiak SE (1998) ENSO theory. J Geophys Res 103(C7):14261–14290. doi;10.1029/97JC03424

Nitta T (1987) Convective activities in the tropical western Pacific and their impact on the Northern Hemisphere summer circulation. J Meteor Soc Jpn 65:373–390

Rajagopalan B, Cook E, Lall U, Ray BK (2000) Spatiotemporal variability of ENSO and SST teleconnections to summer drought over the United States during the twentieth century. J Clim 13:4244–4255

Rasmusson E (1991) Observational aspects of ENSO cycle teleconnections. In: Glantz MH, Katz RW, Nichols N (eds) Teleconnections linking worldwide climate anomalies. Cambridge University Press, Cambridge, pp 309–343

Rasmusson EM, Carpenter TH (1982) Variation in tropical sea surface temperature and surface wind fields associated with the Southern Oscillation/El Niño. Mon Wea Rev 110:354–384

Rayner NA, Parker DE, Horton EB, Folland CK, Alexander LV, Rowell DP, Kent EC, Kaplan A (2003) Global analyses of SST, sea ice and night marine air temperature since the late nineteenth century. J Geophys Res 108. doi:10.1029/2002JD002670

Rogers KB, Friederiches P, Latif M (2004) Tropical Pacific decadal variability and its relation to decadal modulations of ENSO. J Clim 17:3761–3774

Ropelewski CF, Halpert MS (1986) North American precipitation and temperature patterns associated with the El Niño/Southern Oscillation (EMSO). Mon Wea Rev 114:2352–2362

Ropelewski CF, Halpert MS (1996) Quantifying southern oscillation-precipitation relationships. J Clim 9:1043–1059

Saunders MA, Chandler RE, Merchant CJ, Roberts FP (2000) Atlantic hurricanes and NW Pacific typhoons: ENSO spatial impacts on occurrence and landfall. Geophys Res Lett 27:1147–1150

Seager R, Kushnir Y, Herweijer C, Niak N, Velez J (2005) Modeling of tropical forcing of persistent droughts and pluvials over western North America: 1856–2000. J Clim 18:4065–4088

Shukla J, Wallace JN (1983) Numerical simulation of the atmospheric response to equatorial Pacific sea surface temperature anomalies. J Atmos Sci 40:1613–1630

Slingo JM, Annamalai H (2000) 1997: the El Niño of the century and the response of the Indian summer monsoon. Mon Wea Rev 128:1778–1797

Tanaka HL, Ishizaki N, Kitoh A (2004) Trend and interannual variability of Walker, monsoon and Hadley circulations defined by velocity potential in the upper troposphere. Tellus 56A:250–269

Tao S, Chen L (1987) A review of recent research on the East Asian summer monsoon. In: Chang C-P, Krishnamurti TN (eds) Monsoon meteorology. Oxford University Press, China, pp 60–92

Thompson CJ, Battisti DS (2000) A linear stochastic dynamical model of ENSO. Part I: model development. J Clim 13:2818–2832

Ting MF, Wang H (1997) Summer US precipitation variability and its relationship to Pacific sea surface temperature. J Clim 10:1853–1873

Tozuka T, Yamagata T (2003) Annual ENSO. J Phys Oceanogr 33:1564–1578

Trenberth KE (1997) The definition of El Niño. Bull Am Meteor Soc 78:2771–2777

Trenberth KE, Hoar TJ (1996) The 1990–1995 El Niño-Southern Oscillation event: longest on record. Geophys Res Lett 23:57–60

Trenberth KE, Stepaniak DP (2001) Indices of El Niño evolution. J Clim 14:1697–1701

Vera C, Silvestri G, Barros V, Carril A (2004) Differences in El Niño response over the Southern Hemisphere. J Clim 17:1741–1753

Wakabayashi S, Kawamura R (2004) Extraction of major teleconnection patterns possibly associated with the anomalous summer climate in Japan. J Meteor Soc Jpn 82:1577–1588

Waliser DE, Gautier C (1993) A satellite-derived climatology of the ITCZ. J Clim 6:2162–2174

Wallace JM, Gutzler DS (1981) Teleconnections in the geopotential height field during the Northern Hemisphere winter. Mon Wea Rev 109:784–812

Wallace JM, Rasmusson EM, Mitchell TP, Kousky VE, Sarachik ES, von Storch H (1998) On the structure and evolution of ENSO-related climate variability in the tropical Pacific: lessons from TOGA. J Geophys Res 103(C7):14241–14260. doi:10.1029/97JC02905

Wang B, An SI (2002) A mechanism for decadal changes of ENSO behavior: roles of background wind changes. Clim Dyn 18:475–486

Wang B, Fan Z (1999) Choice of south Asian summer monsoon indices. Bull Am Meteor Soc 80:629–638

Wang B, Lin H (2002) Rainy season of the Asian-Pacific summer monsoon. J Clim 15:386–396

Wang Y, Yasunari T (1994) A diagnostic analysis of the wave train propagating from high-latitudes to low-latitudes in early summer. J Meteor Soc Japan 72:269–279

Wang B, Wu R, Lau KM (2001) Interannual variability of the Asian summer monsoon: contrasts between the Indian and the western North Pacific-East Asian monsoons. J Clim 14:4073–4090

Weng HY, Lau KM (1994) Wavelets, period doubling, and time-frequency localization with application to organization of convection over the tropical western Pacific. J Atmos Sci 51:2523–2541

Weng HY, Lau KM, Xue YK (1999) Multi-scale summer rainfall variability over China and its long-term link to global sea surface temperature variability. J Meteor Soc Jpn 77:845–857

Weng HY, Sumi A, Takayabu YN, Kimoto M, Li C (2004) Interannual–interdecadal variation in large-scale atmospheric circulation and extremely wet and dry summers in China/Japan during 1951–2000. Part I: spatial patterns. J Meteor Soc Jpn 82:775–788

Xie SP (1995) Interaction between the annual and interannual variations in the equatorial Pacific. J Phys Oceanogr 25:1930–1941

Yamagata T, Behera SK, Luo JJ, Masson S, Jury MR, Rao SA (2004) Coupled ocean-atmosphere variability in the tropical Indian Ocean. In: Wang C, Xie SP, Carton A (eds) Earth's climate: the ocean–atmosphere interaction. Geophys Monogr 147, Amer Geophys Union, pp 189–211

Yang H, Sun S (2003) Longitudinal displacement of the subtropical high in the western Pacific in summer and its influence. Adv Atmos Sci 20:921–933

Yin X, Gruber A, Arkin P (2004) Comparison of the GPCP and CMAP merged gauge-satellite monthly precipitation products for the period 1979–2001. J Hydrometeor 5:1207–1222

Yu Z, McCreary P Jr (2004) Assessing precipitation products in the Indian Ocean using an ocean model. J Geophys Res 109:C05013. doi:10.1029/2003JC002106

Zebiak SE, Cane MA (1987) A model El Niño Southern Oscillation. Mon Wea Rev 115:2262–2278

Zhang Y, Wallace JM, Battisti DS (1997) ENSO-like interdecadal variability: 1900–93. J Clim 10:1004–1020

Zhou JY, Lau KM (2001) Principal modes of interannual and decadal variability of summer rainfall over South America. Int J Climatol 21:1623–1644